Mechanical Reshaping of Inorganic Nanostructures with Weak Nanoscale Forces

Sarah M. Rehn[1], Theodor M. Gerrard-Anderson[1], Liang Qiao[1], Qing Zhu[2], Geoff Wehmeyer[2], Matthew R. Jones[,1,3]*

[1] Department of Chemistry, Rice University, Houston, Texas 77005, United States.

[2] Department of Mechanical Engineering, Rice University, Houston, Texas 77005, United States.

[3] Department of Materials Science and NanoEngineering, Rice University, Houston, Texas 77005, United States.

Keywords: nanoplate, post-synthetic modification, nanomechanics, deformation, curvilinear, nanostructure

ABSTRACT

Inorganic nanomaterials are often depicted as rigid structures whose shape is permanent. However, forces that are ordinarily considered weak can exert sufficient stress at the nanoscale to drive mechanical deformation. Here, we leverage van der Waals (VdW) interactions to mechanically reshape inorganic nanostructures from planar to curvilinear. Modified plate deformation theory shows that high aspect ratio 2D particles can be plastically deformed via VdW forces. Informed

by this finding, silver nanoplates were deformed over spherical iron oxide template particles, resulting in distinctive bend contour patterns in bright field (BF) transmission electron microscopy (TEM) images. High resolution (HR) TEM images of deformed areas reveal the presence of highly strained bonds in the material. Finally, we show the distance between two nearby template particles allows for the engineering of several distinct curvilinear morphologies. This work challenges the traditional view of nanoparticles as static objects and introduces methods for post-synthetic mechanical shape control.

MAIN TEXT

Nanoscience is predicated on the idea that properties are dictated by nanoscale structure in the form of particle size and shape.[1] In the case of inorganic systems, structure control is most often exerted either during the synthesis to generate a desired particle morphology, or post-synthesis to site-specifically remove/deposit material or assemble building blocks into superstructures. [2-8] Absent among these strategies is the possibility to physically re-shape or re-form inorganic particles via mechanical forces rather than chemical manipulation.[9-11] Previous reports have investigated the mechanical properties of nanomaterials through nanoindentation and other *in situ* methods.[12-19] However, these approaches are low-throughput, single-particle techniques that are often focused more on measuring mechanical properties rather than exercising structural control. Flexibility has been observed in certain nanostructures, but this is often a consequence of random sample preparation processes.[20-22] The mechanisms driving deformation, their size dependence, and the ability to create new morphologies via flexibility remain unclear.

Here, we show that ubiquitous van der Waals (VdW) interactions, which are often considered weak compared to most nanoscale forces, can be leveraged to mechanically deform inorganic nanostructures as a means of post-synthetic shape control. To explore the feasibility of this method, a mathematical model was developed based on continuum mechanics theories for plate deformation. Using the conclusions from this analysis, we show the ability to control the shape of high aspect ratio silver nanoplates by deforming them over small iron oxide template nanospheres. The local deformation caused by a single template particle can furthermore be used as a structural motif to create several unique curvilinear structures. This work challenges the conventional notion that nanoparticles are rigid objects and introduces a new class of curvilinear nanostructures.

To understand the forces that might result in nanoparticle deformation, we assumed that typically weak VdW interactions could be leveraged in a situation in which plate-shaped particles interacted with a surface, since this geometry maximizes the VdW contact area compared to other particle shapes. Additionally, we chose to work with noble metal nanoparticles as they are known to be particularly ductile and can readily be synthesized into 2D morphologies.[20, 23-25] To probe the response to a mechanical stressor under these conditions, Kirchhoff-Love plate theory was employed, which models the elastic deformation and stress behavior of two-dimensional structures. In this formalism, an equilibrium state of mechanical stress is described by a fourth-order partial differential equation, to which there are few tractable solutions. One of the simpler analytical solutions assumes the axially symmetric deformation of a circular disc under a point load (Fig. 1a, inset). Modifying this solution to account for plastic deformation allowed us to compare the relative strength of VdW interactions and mechanical strain energy experienced by nanoplates (see Supporting Information). Given some reasonable assumptions, this analysis

demonstrates that plates with a thickness of <10 nm and an aspect ratio of ~100 represent a transition point, below which VdW interactions are capable of causing a significant particle shape transformation (Fig. 1a, see Supporting Information). Importantly, these findings hold for several other common inorganic nanomaterial systems (e.g., SiO_2, CdSe) and thus indicate the generalizability of VdW-driven mechanical reshaping (Fig. S12, S13).

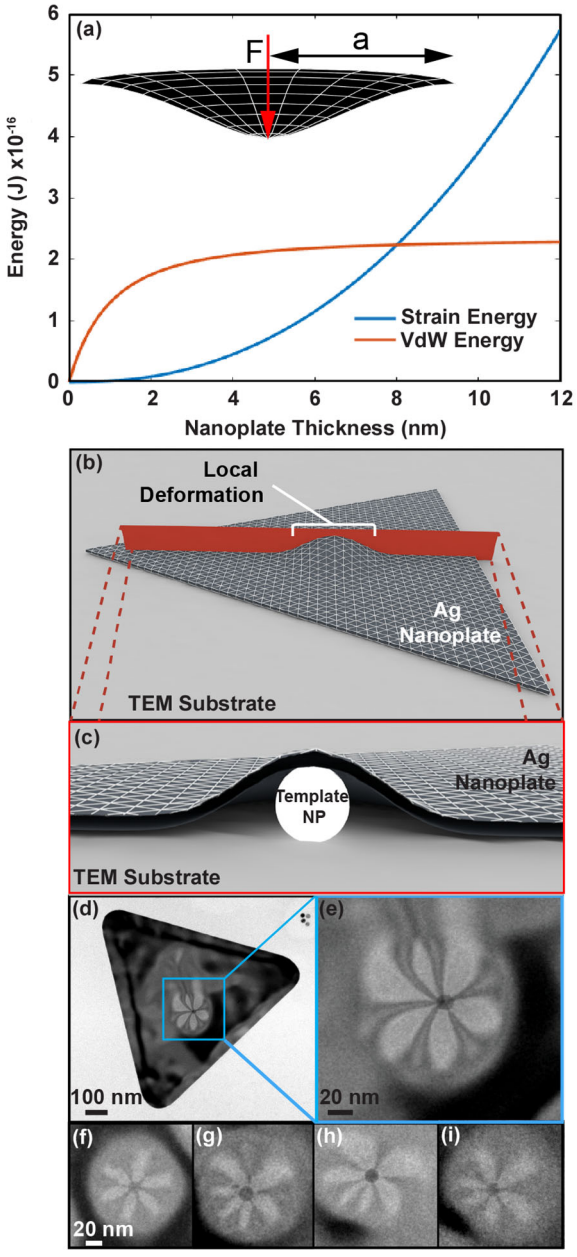

Figure 1. Deformation of thin, silver nanoplates over spherical template particles. (a) Thickness-dependence of the VdW and strain energies as calculated by modified Kirchhoff-Love plate theory. Inset shows the geometry of the strain energy calculation, where *F* is the concentrated force and *a* is the disc radius. Schematics of the (b) top-down and (c) cross sectional view for a nanoplate deformed over a spherical template particle. (d) Representative TEM image of a silver nanoplate deformed over one template nanoparticle, (e) a closer look at the unique bend contour that is observed and f-i) several examples of the bend contours that were seen in every instance of a deformed structure.

Importantly, the mathematical solution describing plate deformation used above can be translated to and investigated in an experimental context. High aspect ratio silver nanoplates of ~8 nm in thickness were synthesized and deformed over spherical iron oxide template particles to mimic a concentrated, axially-symmetric load (Fig. 1a inset, 1b-c). [24, 25] The resulting regions of mechanical strain are evidenced by six-lobed deformation patterns in Bright Field (BF) TEM data (Fig. 1d-e). The unusual pattern of contrast, known as a bend contour, was seen in every instance in which a nanoplate was conformally draped over a spherical template (Fig. 1f-i). Bend contours are a phenomenon that occur when local strain causes nearby crystallographic planes to change their orientation and diffraction condition, resulting in variations in contrast.[20, 26-28] Although bend contours are well-known features of thin TEM samples, they most often extend over large distances and represent gradual changes in the orientation of the material's lattice. The highly symmetric and punctate nature of the bend contours observed in our samples is unusual and points to a localized stress gradient surrounding the spherical particle template. The diameter of these bend contours extended about an order of magnitude larger than the size of the template itself (103 $\pm$ 11 nm, n=228), validating the assumption of a point load in the plate theory model (Fig. 1a).

To confirm whether the 6-fold symmetry of the observed bend contours is related only to an electron diffraction effect and not a real-space morphological feature, we performed selected

area electron diffraction (SAED) and dark-field (DF) TEM analysis. The SAED of a deformed nanoplate exhibits a set of six spots closest to the transmitted beam that represent the 1/3{422} forbidden reflection which is a known feature of structures with internal twinning (Fig. 2a-b).[29] The brighter set of six spots represents the first order diffraction from {220} planes that reveal distinct deformation lobe pairs when selected for in DF TEM imaging (Fig. 2c-h). Therefore, the bend contours that appear in BF TEM images are the convolution of symmetric

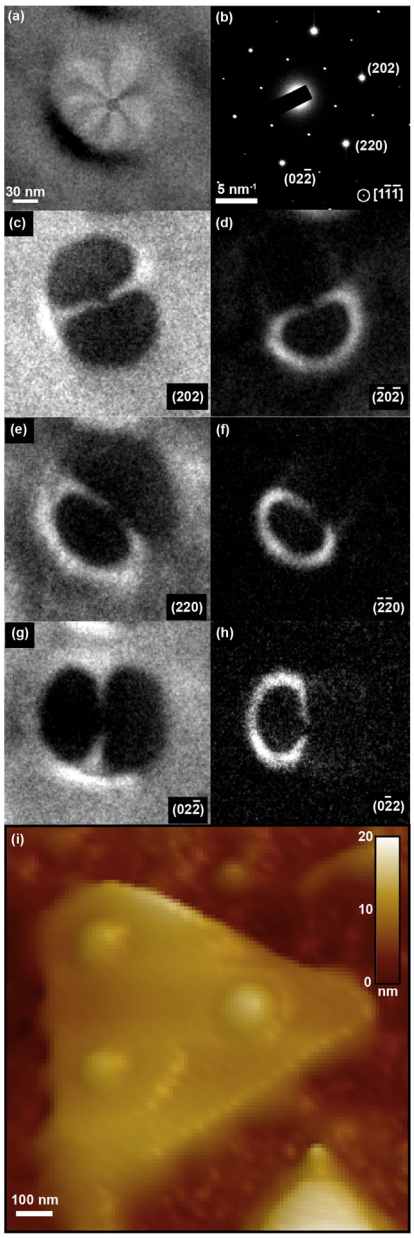

Figure 2. Selected area electron diffraction and dark field analysis of bend contours. (a) BF TEM image of the bend contour used for further analysis. (b) Indexed SAED of the deformed nanoplate revealing the expected 1/3{422} diffraction spots arising from twinning along with first order {220} diffraction spots, and (c-h) DF TEM images corresponding to these spots. (i) 3D AFM topographical map of a nanoplate with axially-symmetric deformed areas.

deformation lobes occurring via {220} planes because the nanoplate is oriented along the $[1\bar{1}\bar{1}]$ zone axis (Fig. 2c-h). Atomic force microscopy (AFM) topographical maps show smooth, axially-symmetric features around template-based deformed regions and are in agreement with bend contour sizes measured by TEM (Fig. 2i, S3). This confirms that the geometry of the proposed model based on plate theory is appropriate for understanding nanoscale shape control.

To further validate these findings, experimental and theoretical results were compared against elastic finite element simulations (COMSOL Multiphysics) using a geometry identical to the Kirchhoff-Love model (Fig. 3). The theory and the simulations utilize some of the same input parameters (e.g., boundary conditions, mechanical constants), but employ different loading conditions and solution methods (see Supporting Information). Experimental height profiles of several deformed nanoplates gathered via AFM measurements (black dots, Fig. 3a), show excellent agreement with the displacement fields generated from both the analytical theory and the finite element simulations (Fig. 3a). While the Kirchhoff-Love theory utilizes a point load to achieve deformation, the simulations explicitly employ the experimental geometry of a small sphere deforming a nanoplate. The agreement between the experimental, simulation-based, and theoretical deflection fields, particularly surrounding the center of the deformed region (x = 0, Fig. 3a), suggests that the approximation of a point load in the theory is reasonable. Quantification of the contact radius between the template particle and nanoplate was determined from simulations to be ~5 nm, an order of magnitude less than the radius of the deformed area itself (see Supporting

Information); this finding further supports the assumption of a point load. Importantly, if instead of considering only the axially-symmetric deformed region, simulations are performed with the entire triangular plate geometry, displacement fields are found to extend over considerably larger length scales (i.e., 200-300 nm) and no longer agree with experiment (green line, Fig. 3a, S18-S21). Since sedimentary forces are negligibly small for particles of nanometer dimensions, this result suggests that only attractive VdW forces can explain the local deformation observed in these structures.

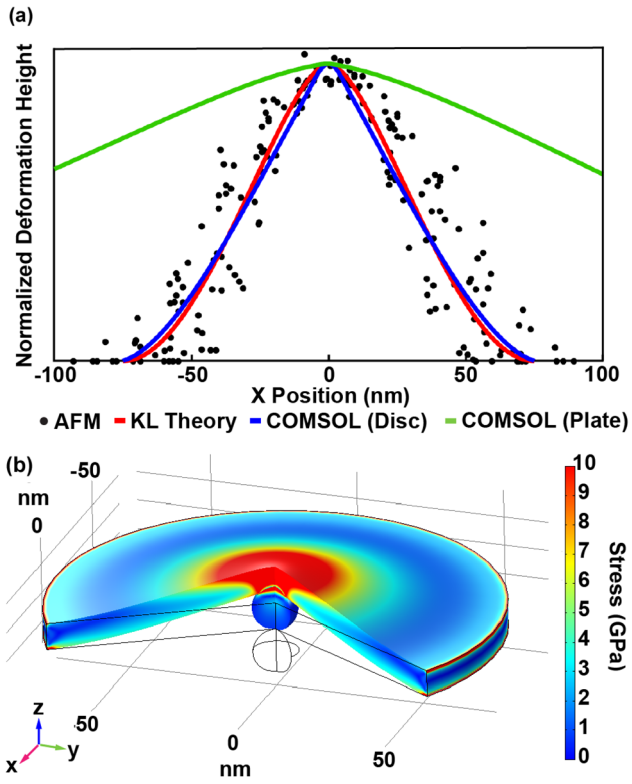

Figure 3. Comparison of experimental and theoretical displacement fields with FEM simulation results. (a) Topographical data from several AFM scans are shown in black. Deflection fields generated from a clamped disc model in both Kirchhoff-Love plate theory (red) and COMSOL (blue) are in good agreement, validating the analytical modeling. Deflection of a triangular nanoplate model in COMSOL (green) do not describe the experiments, showing that plate-substrate clamping due to VdW forces is essential. (b) COMSOL-generated 3D map of von Mises stress (color scale) for a Ag nanoplate with elevated Young's modulus value of 125 GPa. Template-based deformation results in stresses in excess of yield over most of the plate volume.

The simulation results also allow us to generate three-dimensional plots of the internal stresses experienced for plates with a given displacement (Fig. 3b). This information can be used to further understand the structural consequences of VdW-driven nanoparticle shape control by mapping regions for which the yield condition has been surpassed and permanent (plastic) deformation has occurred. Although the bulk yield stress of Ag (54 MPa) is surpassed across the entire volume of the plate, it is well known that metal nanostructures often have higher Young's modulus and yield stress values than their bulk counterparts.[30-35] Quantitative measurements of nanoparticle mechanical constants vary considerably and likely depend sensitively on crystal orientation, dimension, and internal defect structure. Nonetheless, we performed multiple simulations using both bulk and elevated Young's modulus values, appropriate for silver.[30-35] In all cases, the resulting stresses well exceed even the elevated yield stress values (~1 GPa) expected for nanometer-scale silver particles (Fig. 3b, see Supporting Information). This numerical result suggests that plastic deformation is widespread across the volume of the silver nanoplates displaced by template spheres. This conclusion is corroborated by the fact that if plastic deformation is ignored in the Kirchhoff-Love theory, the energy required to achieve the observed displacement far exceeds what is available to the system in the form of VdW or other attractive interactions. Only by modifying the theory to account for the possibility of plastic deformation do we observe agreement between theory and experiment (see Supporting Information).

The curvilinear morphology created by the deformation of nanoplates tilts crystallographic planes and strains the crystal lattice, causing atomic-level distortions. To further understand the role of bond strain and plastic deformation in silver nanoplates, we performed high resolution TEM imaging of regions surrounding the spherical template nanoparticles (Fig. 4). Fast-Fourier Transform (FFT) of these images showed a set of six spots that appear more diffuse in the radial

direction compared to analogous spots in the experimental SAED pattern (Fig. 4b). This reflects the presence of distortion in the atomic Ag lattice, spanning a range of different values. To quantify this, three different rings (red, yellow, cyan) were placed at different radial positions over the diffuse spots in the FFT to denote different degrees of lattice distortion, expressed as a percentage deviation from the unstrained lattice spacing (Fig. 4b and inset). This measurement reveals a deviation of 0-5% or more over the vast majority of the deformed region being imaged. This indicates a degree of lattice distortion significantly above what is ordinarily considered the limit of elastic bond strain, further confirming the necessity of including plastic deformation in the model for nanoplate mechanics.[36-38] Additionally, atomically resolved images show lattice planes and atom positions that are severely distorted with respect to a perfect crystal, indicating numerous broken bonds, defects, and plastic mechanical behavior (Fig. 4c). It is important to note that there exist regions of elastically-strained metal bonds throughout the structure that are consistent with what has been observed to transform a normally inactive noble metal surface to one that can catalyze chemical reactions.[39-41] This suggests that such curvilinear nanostructures might have a high density of active sites for heterogeneous catalysis.

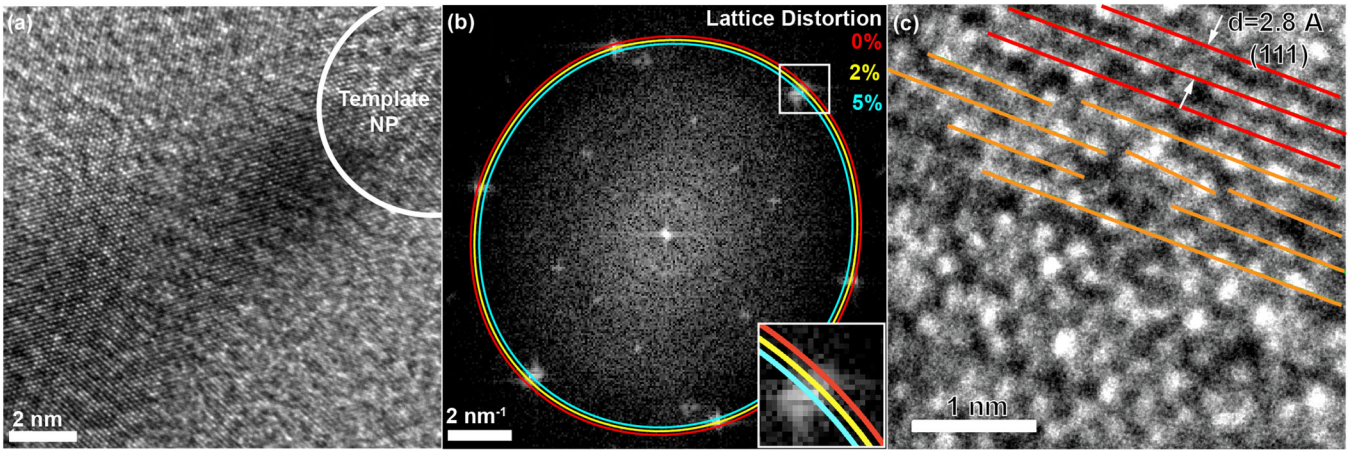

Figure 4. Experimental evidence of severe lattice distortion and strain from plastic deformation. (a) High resolution TEM image of a deformed region and (b) corresponding FFT. The position of bright spots indicate the spacing of {220} lattice planes. Differently colored rings in the FFT correspond to varying atomic spacing. (c) High resolution TEM image showing both normally spaced atomic planes (red) and severe lattice distortions (orange) resulting from deformation.

In traditional nanoscale systems, there are canonical structures from which more complex architectures can be built (e.g., spheres assembled into a superlattice or rods lithographically fabricated into metamaterial arrays).[7, 42] Similarly, we imagined the morphology associated with a single template particle might serve as a basic structural motif for building more complex curvilinear structures. In order to achieve this, we have investigated the topographies that result when two template particles are near one another and deformed regions overlap (Fig. 5). If the parameter *d* is defined as the spacing between nearby template spheres, *d* = 16-31 nm generates a single bend contour that appears slightly larger than one associated with a single template particle (Fig. 5a). Two templates that are separate but closely spaced (*d* = 37-65 nm) show a distorted six-lobed pattern with a region bridging the two particles (Fig. 5b). Interestingly, when *d* increases to ~70-93 nm, a saddle point is observed, consisting of areas of high lattice compression between particles and lattice tension over the template peaks (Fig. 5c). Lastly, templates that are greater than ~94 nm apart display bend contours that are completely decoupled from one another (Fig. 5d). This method relies on the mutual mechanical relaxation of neighboring deformation fields and opens up the possibility for complex curvilinear architectures based on substrate topography rather than lithographic patterning.

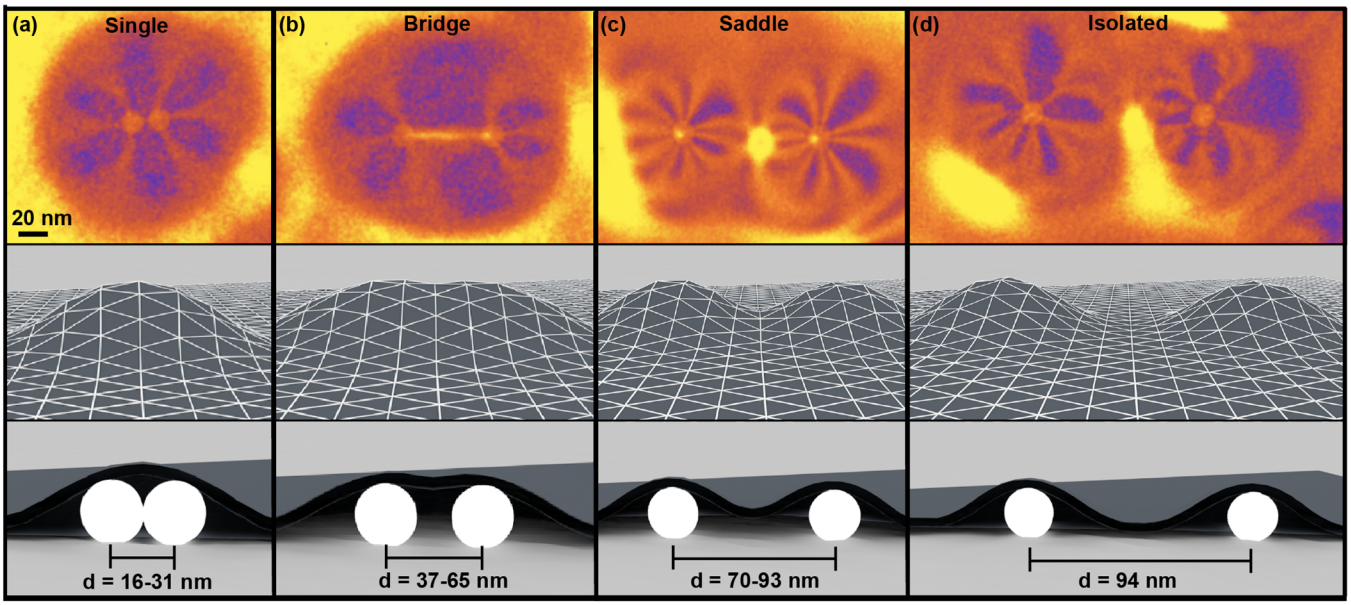

Figure 5. Engineering of coupled curvilinear structures. (a) A single bend contour is observed when two template particles are in physical contact or are extremely close to one another. As two template particles move a distance, *d*, apart from one another, (b) a single distorted bend contour with a bridged region is observed that eventually becomes (c) two distinct contours with a saddle point between them. (d) Eventually, the two templates are far enough apart that isolated bend contours are present with complete structural relaxation between them. A colormap was applied to BF TEM images to enhance differences in contrast for the purpose of analysis (Fig. S5).

In this work we report a simple method for post-synthetic nanoparticle shape modification via mechanical deformation rather than chemical manipulation. Calculations using Kirchhoff-Love plate theory modified to account for plastic deformation create a framework from which to understand the interplay of forces that facilitate this new type of morphological control. Using this in conjunction with simulations and experimental findings, we demonstrate that weak VdW forces can indeed generate enough energy to drive mechanical strain and thereby create a new class of curvilinear structures based on substrate topography. Since these objects would be difficult to generate lithographically, they are expected to result in previously inaccessible electromagnetic modes relevant to the nanooptics community.[43, 44] Furthermore, the gradient of strained bonds in

these materials has implications for their performance or study in catalytic systems.[39-41, 45] Overall, this work demonstrates that inorganic nanoparticles may be thought of as being capable of dynamic structural changes, actuated by simple and ubiquitous nanoscale forces.

ASSOCIATED CONTENT

Supporting information is available free of charge at:

> Experimental details regarding materials and methods, mathematical derivation and calculations, and characterization data.

AUTHOR INFORMATION

Corresponding Author

*Corresponding author. Email:mrj@rice.edu

Author Contributions

The manuscript was written through contributions of all authors. All authors have given approval to the final version of the manuscript.

Funding Sources

Notes

The authors declare no competing financial interest.

ACKNOWLEDGMENT

M. R. J. would like to acknowledge financial support from the Robert A. Welch Foundation (Grant C-1954) and the David and Lucile Packard Foundation (Grant 2018-68049). G.W. and Q.Z. would like to acknowledge funding support from the Robert A. Welch Foundation (Grant

C- 2023). S.M. R. would like to acknowledge financial support from a National Science Foundation Graduate Research Fellowship #1450681. The authors would like to acknowledge financial support from Rice University.

ABBREVIATIONS

BF, bright field; DF, dark field; FFT, fast-Fourier transform; HR, high resolution; SAED, selected area electron diffraction; TEM, transmission electron microscopy; VdW, van der Waals

REFERENCES

1. Mock, J. J.; Barbic, M.; Smith, D. R.; Schultz, D. A.; Schultz, S., Shape Effects in Plasmon Resonance of Individual Colloidal Silver Nanoparticles. *J. Chem. Phys.* **2002,** *116*, 6755-6759.

2. Mulvihill, M. J.; Ling, X. Y.; Henzie, J.; Yang, P., Anisotropic Etching of Silver Nanoparticles for Plasmonic Structures Capable of Single-Particle SERS. *J. Am. Chem. Soc.* **2010,** *132*, 268-274.

3. Rathmell, A. R.; Bergin, S. M.; Hua, Y. L.; Li, Z. Y.; Wiley, B. J., The Growth Mechanism of Copper Nanowires and Their Properties in Flexible, Transparent Conducting Films. *Adv. Mater.* **2010,** *22*, 3558-3563.

4. Singh, G.; Chan, H.; Baskin, A.; Gelman, E.; Repnin, N.; Král, P.; Klajn, R., Self-Assembly of Magnetite Nanocubes into Helical Superstructures. *Science* **2014,** *345*, 1149-1153.

5. Jones, M. R.; Macfarlane, R. J.; Lee, B.; Zhang, J.; Young, K. L.; Senesi, A. J.; Mirkin, C. A., DNA-Nanoparticle Superlattices Formed From Anisotropic Building Blocks. *Nat. Mater.* **2010,** *9*, 913-917.

6. Macfarlane, R. J.; Lee, B.; R., J. M.; Harris, N.; Schatz, G. C.; Mirkin, C. A., Nanoparticle Superlattice Engineering with DNA. *Science* **2011,** *334*, 204-208.

7. Lewis, D. J.; Zornberg, L. Z.; Carter, D. J. D.; Macfarlane, R. J., Single-Crystal Winterbottom Constructions of Nanoparticle Superlattices. *Nat. Mater.* **2020,** *19*, 719-724.

8. Straney, P. J.; Marbella, L. E.; Andolina, C. M.; Nuhfer, N. T.; Millstone, J. E., Decoupling Mechanisms of Platinum Deposition on Colloidal Gold Nanoparticle Substrates. *J. Am. Chem. Soc.* **2014,** *136*, 7873-7876.

9. Kim, Y.; Zhu, J.; Yeom, B.; Prima, M. D.; Su, X.; Kim, J.-G.; Yoo, S. J.; Uher, C.; Kotov, N. A., Stretchable Nanoparticle Conductors with Self-Organized Conductive Pathways. *Nature* **2013,** *500*, 59-63.

10. Kim, Y.; Yeom, B.; Arteaga, O.; Yoo, S. J.; Lee, S.-G.; Kim, J.-G.; Kotov, N. A., Reconfigurable Chiroptical Nanocomposites with Chirality Transfer from the Macro- to the Nanoscale. *Nat. Mater.* **2016,** *15*, 461-468.

11. Gu, X. W.; Ye, X.; Koshy, D. M.; Vachhani, S.; Hosemann, P.; Alivisatos, A. P., Tolerance to Structural Disorder and Tunable Mechanical Behaviour in Self-Assembled Superlattices of Polymer-Grafted Nanocrystals. *Proc. Natl. Acad. Sci.* **2017,** *114*, 2836-2841.

12. Pharr, G. M.; Oliver, W. C., Measurement of Thin Film Mechanical Properties Using Nanoindentation. *MRS Bulletin* **1992,** *17*, 28-33.

13. Panin, A.; Shugurov, A.; Oskomov, K., Mechanical Properties of Thin Ag Films on a Silicon Substrate Studied Using the Nanoindentation Technique. *Phys. Solid State* **2005,** *47*, 2055-2059.

14. Zeng, Z.; Tan, J.-C., AFM Nanoindentation to Quatify Mechanical Properties of Nano- and Micron-Sized Crystal of a Metal Organic Framework Material. *ACS App. Mater. Interfaces* **2017,** *9*, 39839-39854.

15. Lee, C.; Wei, X.; Kysar, J. W.; Hone, J., Measurement of the Elastic Properties and Intrinsic Strength of Monolayer Graphene. *Science* **2008,** *321*, 385-388.

16. Gu, X. W.; Wu, Z.; Zhang, Y.-W.; Srolovitz, D. J.; Greer, J. R., Microstructure versus Flaw: Mechanisms of Failure and Strength in Nanostructures. *Nano Lett.* **2013,** *13*, 5703-5709.

17. Zhang, H.; Lu, Y., Low-Cycle Fatigue Testing of Ni Nanowires Based on a Micro-Mechanical Device. *Exp. Mech.* **2017,** *57*, 495-500.

18. Yu, Q.; Legros, M.; Minor, A. M., In situ TEM Nanomechanics. *MRS Bulletin* **2015,** *40*, 62-70.

19. Patil, R. P.; Doan, D.; Aitken, Z. H.; Chen, S.; Kiani, M. T.; Barr, C. M.; Hattar, K.; Zhang, Y.-W.; Gu, X. W., Hardening in Au-Ag nano boxes from Stacking Fault-Dislocation Interactions. *Nat. Commun.* **2020,** *11*, 2923.

20. Rodríguez-González, B.; Pastoriza-Santos, I.; Liz-Marzán, L. M., Bending Contours in Silver Nanoprisms. *J. Phys. Chem. B* **2006,** *110*, 11796-11799.

21. De, S.; Higgins, T. M.; Lyons, P. E.; Doherty, E. M.; Nirmalraj, P. N.; Blau, W. J.; Boland, J. J.; Coleman, J. N., Silver Nanowire Networks as Flexible, Transparent, Conducting Films: Extremely High DC to Optical Conductivity Ratios. *ACS Nano* **2009,** *3*, 1767-1774.

22. Lee, J.; Lee, P.; Lee, H.; Lee, D.; Lee, S. S.; Ko, S. H., Very Long Ag Nanowire Synthesis and its Application in Highly Transparent, Conductive and Flexible Metal Electrode Touch Panel. *Nanoscale* **2012,** *4*, 6408-6414.

23. Mehl, M. J.; Papaconstantopoulos, D. A.; Kioussis, N.; Herbranson, M., Tight-Binding Study of Stacking Fault Energies and the Rice Criterion of Ductility in the FCC Metals. *Phys. Rev. B* **2000,** *61*, 4894-4897.

24. Zhang, Q.; Li, N.; Goebl, J.; Lu, Z.; Yin, Y., A Systematic Study of the Synthesis of Silver Nanoplates: Is "Citrate" a Magic Reagent? *J. Am. Chem. Soc.* **2011,** *133*, 18931-18939.

25. Liu, X.; Li, L.; Yang, Y.; Yin, Y.; Gao, C., One-Step Growth of Triangular Silver Nanoplates with Predictable Sizes on a Large Scale. *Nanoscale* **2014,** *6*, 4513-4516.

26. Carlton, C. E.; Ferreira, P. J., In Situ TEM Nanoindentation of Nanoparticles. *Micron* **2012,** *43*, 1134-1139.

27. Sun, H.; Pan, X., Microstructure of ZnO Shell on Zn Nanoparticles. *J. Mater. Res.* **2004,** *19*, 3062-3067.

28. Cuberes, M. T.; Stegemann, B.; Kaiser, B.; Rademann, K., Ultrasonic Force Microscopy on Strained Antimony Nanoparticles. *107* **2007**, 1053-1060.

29. Germain, V.; Li, J.; Ingert, D.; Wang, Z. L.; Pileni, M. P., Stacking Faults in Formation of Silver Nanodisks. *J. Phys. Chem. B* **2003,** *107* (34), 8717-8720.

30. Wu, B.; Heidelberg, A.; Boland, J. J.; Sader, J. E.; Sun, X. M.; Li, Y., Microstructure-Hardened Silver Nanowires. *Nano Lett.* **2006**, *6*, 468-472.

31. Zhang, S. B., Microstructure- and Surface Orientation- Dependent Mechanical Behaviors of Ag Nanowires Under Bending. *Comput. Mater. Sci.* **2014**, *95*, 53-62.

32. Gao, Y.; Fu, Y.; Sun, W.; Sun, Y.; Wang, H.; Wang, F.; Zhao, J., Investigation on the Mechanical Behavior of Fivefold Twinned Silver Nanowires. *Comput. Mater. Sci.* **2012**, *55*, 322-328.

33. Vlassov, S.; Polyakov, B.; Dorogin, L. M.; Antsov, M.; Mets, M.; Umalas, M.; Saar, R.; Lõhmus, R.; Kink, I., Elasticity and Yield Strength of Pentagonal Silver Nanowires: In Situ Bending Test. *Mater. Chem. Phys.* **2014**, *143*, 1026-1031.

34. Li, X.; Gao, H.; Murphy, C. J.; Caswell, K. K., Nanoindentation of Silver Nanowires. *Nano Lett.* **2003**, *3*, 1495-1498.

35. Kiani, M. T.; Patil, R. P.; Gu, X. W., Dislocation Surface Nucleation in Surfactant-Passivated Metallic Nanocubes. *MRS Commun.* **2019**, *9*, 1029-1033.

36. Zhang, J.; Tang, Y.; Lee, K.; Ouyang, M., Nonepitaxial Growth of Hybrid Core-Shell Nanostructures with Large Lattice Mismatches. *Science* **2010,** *327*, 1634-1638.

37. Yao, Y.; He, D. S.; Lin, Y.; Feng, X.; Wang, X.; Yin, P.; Hong, X.; Zhou, G.; Wu, Y.; Li, Y., Modulating FCC and HCP Ruthenium on the Surface of Palladium-Copper Allow Through Tunable Lattice Mismatch. *Angewandte Chemie* **2016,** *128*, 5591-5595.

38. Diao, J.; Gall, K.; Dunn, M. L., Yield Strength Asymmetry in Metal Nanowires. *Nano Lett.* **2004,** *4*, 1863-1867.

39. Kim, J.-S.; Kim, H.-K.; Kim, S.-H.; Kim, I.; Yu, T.; Han, G.-H.; Lee, K.-Y.; Lee, J.-C.; Ahn, J.-P., Catalytically Active Au Layers Grown on Pd Nanoparticles for Direct Synthesis of H_2O_2: Lattice Strain and Charge-Transfer Perspective Analyses. *ACS Nano* **2019,** *13* (4), 4761-4770.

40. Bueno, S. L. A.; Gamler, J. T. L.; Skrabalak, S. E., Ligand-Guided Growth of Alloyed Shells on Intermetallic Seeds as a Route Toward Multimetallic nano catalysts with Shape-Control. *Chem. Nano Mat.* **2020,** *6*, 783-789.

41. Mukherjee, D.; Gamler, J. T. L.; Skrabalak, S. E.; Unocic, R. R., Lattice Strain Measurement of Core@Shell Electrocatalysts with 4D Scanning Transmission Electron Microscopy Nanobeam Electron Diffraction. *ACS Catal.* **2020,** *10*, 5529-5541.

42. Pryce, I. M.; Kelaita, Y. A.; Aydin, K.; Atwater, H. A., Compliant Metamaterials for Resonantly Enhanced Infrared Absorption Spectroscopy and Refractive Index Sensing. *ACS Nano* **2011,** *5* (10), 8167-8174.

43. Prodan, E.; Radloff, C.; Halas, N. J.; Nordlander, P., A Hybridization Model for the Plasmon Resonance of Complex Nanostructures. *Science* **2003,** *302*, 419-422.

44. Wang, H.; Brandl, D. W.; Nordlander, P.; Halas, N. J., Plasmonic Nanostructures: Artificial Molecules. *Acc. Chem. Res.* **2007,** *40*, 53-62.

45. Sneed, B. T.; Young, A. P.; Tsung, C.-K., Building up Strain in Colloidal Metal Nanoparticle Catalysts. *Nanoscale* **2015,** *7*, 12248-12265.